HHS Public Access

Author manuscript

Dent Mater. Author manuscript; available in PMC 2018 October 01.

Published in final edited form as:

Dent Mater. 2017 October ; 33(10): 1069–1074. doi:10.1016/j.dental.2017.07.005.

The interrelationship of microstructure and hardness of human coronal dentin using reference point indentation technique and micro-Raman spectroscopy

Rasoul Seyedmahmoud[a], **Jacob D. McGuire**[a], **Yong Wang**[a,b,*], **Ganesh Thiagarajan**[c], and **Mary P. Walker**[a,b,**]

[a]Department of Oral and Craniofacial Sciences, School of Dentistry, University of Missouri-Kansas City, MO

[b]Center of Excellence in Musculoskeletal and Dental Tissues, University of Missouri-Kansas City, MO

[c]Department of Civil and Mechanical Engineering, School of Computing and Engineering, University of Missouri-Kansas City, MO

Abstract

Objectives—The aim of this paper is to determine the interrelationship between the microstructure--in terms of chemical composition and crystallinity--to the microhardness of coronal dentin.

Methods—Dentin microhardness was tested by a novel reference point indenter and compared to the traditional Knoop hardness method. Micro-Raman spectroscopy was used to determine the chemical composition and crystallinity of dentin.

Results—From the occlusal groove to the border of the coronal pulp chamber, dentin hardness decreased from superficial dentin (SD) to deep dentin (DD). Mineral/organic matrix ratios (phosphate/C-H and phosphate/amide I) also decreased from SD to DD; however, this change was significant ($P<0.05$) in the phosphate/amide I ratio only. The phosphate/carbonate ratio decreased significantly by varying position from SD to DD. The degree of the crystallinity, as measured by the full width at half maximum (FWHM) of the peak at 960cm^{-1}, decreased significantly going from superficial to deep dentin.

Significance—For the first time, the interrelationship between the microstructure and the mechanical properties of coronal dentin was determined by using the novel reference point indentation technique and micro-Raman spectroscopy. We hypothesize that the decrease in

Corresponding Authors: Dr. Mary P. Walker** and Dr. Yong Wang*, Department of Oral and Craniofacial Sciences, Center of Excellence in Musculoskeletal and Dental Tissues, University of Missouri-Kansas City School of Dentistry, 650 East 25th St, Kansas City, MO 64108, walkermp@umkc.edu; wangyo@umkc.edu, **Phone: +1-816-235-2825, *Phone: (816) 235-2043, Fax: +1-816-235-5524.

Conflict of Interest: none.

hardness from superficial to deep dentin can potentially be explained by decreased mineral content and increased carbonate content, which is also associated with decreased crystallinity. Collectively, there is a positive association between dentin hardness and mineral content and a negative association between dentin hardness and carbonate content.

Keywords

Dentin; Hardness; Chemical composition; Reference point indentation; Knoop hardness; Micro-Raman spectroscopy

1. Introduction

Tooth dentin is a hierarchical biocomposite composed of different structural elements, such as, dentinal tubules, highly-mineralized peritubular, intertubular dentin that is composed of type I collagen, and dentinal fluid [1]. The distribution of structural elements from superficial dentin, i.e., by the dentin-enamel junction (DEJ), to deep dentin, i.e., near the border of the coronal pulp chamber, results in an anisotropic biocomposite in which properties vary by location. Studies that have evaluated the structure and material properties of dentin suggest that the mechanical properties of dentin are dependent on its internal structure, composition, and external environment [2–4].

It is vital to understand the mechanical properties of the dentin in order to determine its structure-property relationships. Several informative reviews in the context of mechanical properties of human tooth are available describing different techniques and results [5–7]. Among these properties of human teeth, hardness is routinely reported in the literature. This is likely due to available testing methods. Hardness tests are fast, simple, user-friendly and can be correlated to other mechanical properties, e.g. Young's modulus [8], thin-film bond strength [9] and shear bond strength [10]. Hardness can also be determined by micro- and nano-indentation techniques [8, 10, 11]. However, reported hardness values vary, which may be due to the innate variability of human teeth and/or testing methods. To this end, studies have been addressing the precision and accuracy of the reported hardness values by either upgrading methods or evaluating new techniques [12, 13]. Recently, the reference point indentation (RPI) technique has gained widespread interest as a microindentation tester in characterizing mechanical properties of bone [14]. Similar to the traditional microindentation hardness tester, RPI can be used to measure microhardness. However, the capability and accuracy of this technique in evaluating microhardness of coronal dentin is unclear. To this end, to validate the micro-scale hardness obtained by the RPI technique, the Knoop hardness tester was included as a reference.

The purpose of this study was to determine the interrelationship between the microstructure--in terms of chemical composition and crystallinity--to the microhardness of coronal dentin. Dentin microhardness was tested by using a novel reference point indenter technique compared to the traditional Knoop hardness method. Micro-Raman spectroscopy was used to characterize the chemical composition and crystallinity of dentin.

2. Materials and Methods

2.1. Preparation of dentin specimens

Twenty-six, extracted third molars from individuals 17–21 years old were collected according to a protocol approved by an institutional board (IRB13-924NHS). Because these extracted teeth were not associated with any patient identifiers, their use in the project was categorized as not human subject research by the IRB. Excess soft tissue was removed and the teeth were stored at 4°C in phosphate buffered saline (PBS, pH 7.4) with 0.002% sodium azide.

A slow-speed, water-cooled diamond saw (Buehler Ltd, Lake Bluff, IL, USA) was utilized to remove the roots, parallel to the occlusal table, approximately 5 mm below the cemento-enamel junction (CEJ). For hardness testing, 20 of the tooth crowns were sectioned bucco-lingually to create, two, paired 2-mm-thick sections from each tooth. Those forty sections were embedded in cold-curing epoxy resin (EpoxiCure 2, Buehler, Lake Bluff, IL, USA) and polished with a motorized wheel (Metaserv, Buehler, Lake Bluff, IL, USA) using decreasing grit-sized waterproof silicon carbide, polishing cloth papers, and finished with diamond paste. Specimens were washed ultrasonically after each step to remove any surface debris. For micro-Raman spectroscopy, the remaining six tooth crowns were sectioned bucco-lingually to generate one 2-mm-thick section from each tooth. Before analysis, the sections were sequentially polished under water using 600- and 1200-grit SiC paper.

2.2. Hardness Test

Using the embedded sections, the hardness of coronal dentin was measured along a reproducible line starting at the occlusal groove to the border of the coronal pulp chamber; two locations were designated: superficial dentin (SD), 200-μm from the DEJ; and deep dentin (DD), 200-μm above the coronal pulp chamber boundary. A BioDent RPI technique and traditional Knoop hardness method were used respectively with one of the paired sections from twenty teeth.

A Knoop hardness test was performed using a Wilson Hardness Tukon 1202 (Buehler, Lake Bluff, IL, USA). Knoop hardness numbers (KHN) were calculated as the load divided by the length of the longest diagonal:

$$\mathrm{KHN}=14.229\,\frac{P}{d^2}$$

Where P is the applied load and d is the length of the longest diagonal measured from a secondary electron microscopy image. Knoop indentations were performed at two load levels (0.1-or 0.5-N) with a 10-second dwell time.

BioDent hardness numbers (BHN) were obtained using a BioDent RPI (Active Life Scientific, Santa Barbara, CA, USA) with Bone Probe 1 using two load levels (2-or 3-N) with a 10-second dwell time. This probe assembly features a sharp, beveled edge reference probe that anchors the probe assembly to the dentin surface. BHN were calculated by

dividing the applied force by the area of the conical indentation pattern formed by the test probe and is given as:

$$\mathrm{BHN}=\frac{\mathrm{P}}{\pi \mathrm{r}\sqrt{\mathrm{r}^2+\mathrm{h}^2}}$$

Where P is the applied load, r is a radius of the indentation calculated from the SEM image, and h is the indentation distance as reported by the instrument.

2.3. Scanning Electron Microscopy

In order to generate hardness values, scanning electron microscopy (SEM) images (FEI-XL30, FEI Company, Hillsboro, OR) were collected on the platinum-gold coated tooth sections using 5.00kV at 1000x magnification and secondary electron detector (SE). To calculate the hardness numbers, the length of the longest diagonal Knoop indentations and radius of the BioDent indentations were measured with image analysis software (Image J; National Institutes of Health; Bethesda, MD). Mean hardness numbers and standard deviations were calculated at each dentin location at each load for each technique. Data was compared as a function of technique, load and dentin location using an analysis of variance (ANOVA) with statistical significance set at α=0.05.

2.4. Micro-Raman Spectroscopy

To determine the microstructure-mechanical relationship of SD and DD, a LabRam HR 800 Raman spectrometer (Horiba Jobin Yvon, Eddison, NJ, USA) with monochromatic radiation emitted by a He-Ne laser (a wavelength of 632.8 nm and excitation power of 20 mW) was used. The spectral information was obtained using the following parameters: 1800 grating, 400-μm confocal hole and 150-μm slit width. Before data collection, the spectra were Raman-shift-frequency calibrated with known lines of silicon.

Using the non-embedded, polished sections from 6 different teeth, for each dentin region (SD and DD), six spectra were acquired (from 800 to 1800cm^{-1}) by focusing the laser beam through a 20X - water immersion objective onto the tooth sections. Labspec 5 software (HORIBA JOBIN YVON) was used to analyze the acquired Raman spectra. To analyze the spectral information, smoothing and manual multiple-point baseline correction was applied to the acquired Raman spectra. Raman data was obtained based on peak intensities of the ν_1 vibration of phosphate at 960cm^{-1} [15], ν_1 vibration of the carbonate group (B type of carbonate) in hydroxyapatite at 1070cm^{-1} [16], δ vibration of C-H band at 1452cm^{-1} [17], and amide I band at 1667cm^{-1} [16]. The mineral-organic matrix ratios (960/1452 and 960/1667cm^{-1}) were calculated by integrating the area under the peaks to analyze differences in the chemical composition in SD and DD [17]. The phosphate/carbonate ratio was obtained similarly to analyze differences in the mineral composition at SD and DD [18]. To assess any differences in degree of the crystallinity at SD and DD, the full-width at half maximum (FWHM) of phosphate peak at 960cm^{-1} was measured [16]. An ANOVA (α=0.05) was used to determine any statistical differences between the mineral/organic matrix and phosphate/carbonate ratios and FWHM for 960 cm^{-1} at varying dentin positions.

3. Results

At each level of load, BHN at SD were significantly higher than DD, while KHN were not significantly different between SD and DD at each load (Figure 1). Notably, the standard deviations associated with KHN were relatively higher compared to BHN.

Scanning electron microscopy revealed two different microindentation patterns. An elongated diamond-shaped indent was produced by the Knoop indenter, and a conical-shaped indent was created by the BioDent RPI instrument (Figure 2). At each level of load, BioDent RPI indentations were larger and deeper in DD versus SD, whereas the elongated rhombic Knoop indentations size didn't change by dentin location.

Representative Raman spectra obtained from SD and DD are shown in Figure 3. The mean and standard deviation of the phosphate/C-H (960/1452cm^{-1}), phosphate/amide I (960/1667cm^{-1}), phosphate/carbonate (960/1070cm^{-1}) ratios and the FWHM of phosphate at 960 cm^{-1} are presented in Table 1. By varying position from SD to DD, all of the ratios decreased. This reduction, however, was only significant ($P<0.05$) for the phosphate/C-H and phosphate/carbonate ratios. At the deep dentin location, the FWHM of phosphate at 960cm^{-1} increased significantly ($P<0.05$) compared to superficial dentin.

4. Discussion

To our knowledge, this is the first study to evaluate the capability and accuracy of the novel BioDent RPI technique to measure the microhardness of coronal dentin. Our values for both mean BHN and KHN are in accordance with previously reported values of dentin microhardness [19, 20]. Moreover, similar to the previous study [7], BioDent RPI technique confirmed that the microhardness of dentin decreased apically toward deep dentin. The typical indentation patterns obtained from Knoop and BioDent RPI at SD and DD are shown in Figure 2. The standard deviation associated with Knoop hardness numbers showed high variability similar to previous studies [19, 20]. Interestingly, variability was less pronounced in dentin microhardness results obtained by BioDent RPI (Figure 1).

Within the test load ranges, no significant Knoop hardness-load dependency was detected, at either SD or DD ($P>0.05$). Interestingly, at each location, the BioDent hardness values showed a significant load dependency. These differences are likely due to the indentation size effect (ISE) [20, 21]. There are two types of ISE: 1) normal ISE, a reduction in hardness occurs where indentation load is increased; and 2) reverse ISE, which is associated with increasing hardness when indentation load is increased [20]. As reported in a previous study [22], for the Knoop hardness test, normal ISE at SD and reverse ISE at DD occurred. For the BioDent RPI test, however, normal ISE at DD and reverse ISE at SD was observed. The ISE can be influenced by two factors. First, technical limitations, e.g., resolution of the optical system, or operator errors could affect the accuracy of the hardness measurement [21]. In this study, to increase the accuracy of the microhardness measurement and to limit introduction of an external variable, every load level of the experiment was performed by the same investigator. High resolution SEM micrographs were implemented to precisely measure the size of each indentation. Second, elastic recovery of the indentations [20, 21,

23] may also affect ISE. Likewise, it was reported that the time and speed of elastic recovery after indentation and elastic-plastic deformation during dwelling time, introduces an additional uncertainty in the accuracy of the hardness measurement [20]. Visco-elastic deformation affects the indentation size measurement during elastic recovery after indenter removal [20] and also by increasing the depth of the impression during loading [24]. Interestingly, the novel BioDent RPI technique is less affected by the elastic recovery property of the material. The reason is that with the BioDent RPI, the indentation distance is measured under testing load. Moreover, the minimum testing load in BioDent RPI technique, 2 N, is relatively higher than testing loads used with the Knoop hardness test. The higher loading force with BioDent RPI leads to deeper surface penetration and thus, makes this technique less sensitive to the surface conditions. This could explain the lower standard deviation associated with BHN. Altogether, our results suggest that the novel BioDent RPI is a consistent and reproducible technique for analyzing dentin microhardness.

To determine the interrelationship between the chemical composition and microhardness of dentin, the mineral/organic matrix ratios were analyzed. At superficial dentin both phosphate/C-H (960/1452cm^{-1}) and phosphate/amide I (960/1667cm^{-1}) ratios demonstrated a higher ratio of mineral/organic matrix compared to the deep dentin (Table 1). However, only the phosphate/amide I ratio at SD was significantly higher compared to DD. In other words, superficial dentin near the DEJ is composed of more mineral compared to deep dentin near the pulp chamber border. This suggests that a positive relationship exists between the mineral content and hardness of dentin. In support of our findings, the hardness of dentin has been previously reported to be dependent on its mineral content and the reduction in dentin hardness is directly linked to the mineral content [2]. However, the previous investigators correlated the mechanical properties of dentin measured by an ultra-micro indentation system to the mineral content determined by backscattered scanning electron imaging [2].

To establish a correlation between the mineral composition/quality (i.e., the degree of the crystallinity and dentin hardness), FWHM of phosphate at 960cm^{-1} and the phosphate/carbonate ratio were calculated. Crystallinity is defined as the degree of long range order in materials and strongly affects the mechanical properties [25]. The increase in degree of crystallinity at 960 cm^{-1} is indicated by the presence of hydroxyapatite crystals, which suggest a relatively lower degree of imperfection and substitutions [26].

In this study, the degree of crystallinity was evaluated by calculating the FWHM of the ν_1 vibration band of phosphate at 960cm^{-1} comparing SD to DD. This index reflects the crystallographic structure, since narrower peaks suggest less structural variation in bond distance and angles [30]. In general, a well-crystallized apatite has a narrow peak, while a crystal with high carbonate content has a broader peak [31]. Our results showed that there was a significant increase ($P<0.05$) in FWHM indicating a decrease in crystallinity going from SD to DD.

Moreover, it was previously reported that the presence of a prominent carbonate band around 1070 cm^{-1} correlated with the degree of carbonate substitution in the lattice structure of apatite [27]. It was also reported that there is a significant negative correlation between

carbonate content and associated crystallinity with the hardness of bone [28] and human enamel [29]. Based on the current micro-Raman results, the phosphate/carbonate ratio significantly decreased from 10.65±1.13 to 7.69±126 cm^{-1} between SD and DD dentin locations. These results suggest that DD is composed of more carbonate than SD. Altogether, our results suggest that as carbonate content increases, the crystallinity of dentin correspondingly decreases.

Our results support that dentin is a gradient biocomposite material and its mechanical properties and microstructure vary by location. The novel BioDent RPI and traditional Knoop hardness tests suggest that the hardness of dentin decreased by varying the location from SD to DD. The BioDent RPI technique is less affected by the dentin surface condition and has the potential to generate more consistent hardness values as compared to the traditional Knoop indenter. Micro-Raman spectroscopy analysis revealed that the chemical composition of dentin changes as a function of dentin location. Our results demonstrate that superficial dentin contained more mineral content and relatively deep dentin contained more organic matrix and carbonate content. Moreover, the FWHM of phosphate at 960 cm^{-1} increased from SD to DD. Collectively, these results suggests a positive relationship a between dentin hardness and mineral content, while there is a negative relationship between dentin hardness and carbonate content, which is linked to decreased mineral crystallinity.

5. Conclusion

To our knowledge, this is the first study to evaluate the capability and accuracy of the novel BioDent RPI technique to measure the hardness of coronal dentin. Moreover, for the first time micro-Raman spectroscopy and Reference point indentation technique were used to determine the interrelationship between the microstructure and hardness of dentin. These results demonstrate that hardness decreases from superficial to deep dentin. This can potentially be explained by the contributing effect of decreasing mineral content and increased carbonate content that would be associated with decreased crystallinity from superficial to deep dentin.

Acknowledgments

This work was supported by NIH/NIDCR grant R01DE021462.

Abbreviations

RPI	reference point indenter
PBS	phosphate buffered saline
CEJ	cementoenamel junction
SD	superficial dentin
DD	deep dentin
DEJ	dentin-enamel junction

KHN	Knoop hardness numbers
BHN	BioDent hardness numbers
ANOVA	analysis of variance
SEM	scanning electron microscopy
SE	secondary electron detector
FWHM	full-width at half maximum
ISE	indentation size effect

References

1. Ziskind D, Hasday M, Cohen SR, Wagner HD. Young's modulus of peritubular and intertubular human dentin by nano-indentation tests. J Struct Biol. 2011; 174:23–30. [PubMed: 20850543]
2. Angker L, Nockolds C, Swain MV, Kilpatrick N. Correlating the mechanical properties to the mineral content of carious dentine--a comparative study using an ultra-micro indentation system (UMIS) and SEM-BSE signals. Arch Oral Biol. 2004; 49:369–78. [PubMed: 15041484]
3. Guidoni G, Denkmayr J, Schöberl T, Jäger I. Nanoindentation in teeth: influence of experimental conditions on local mechanical properties. Philosophical Magazine. 2006; 86:5705–14.
4. Cohen SR, Apter N, Jesse S, Kalinin S, Barlam D, Peretz AI, et al. AFM Investigation of Mechanical Properties of Dentin. Israel Journal of Chemistry. 2008; 48:65–72.
5. Yahyazadehfar M, Ivancik J, Majd H, An B, Zhang D, Arola D. On the Mechanics of Fatigue and Fracture in Teeth. Applied Mechanics Reviews. 2014; 66:030803--19.
6. Bertassoni LE. Dentin on the nanoscale: Hierarchical organization, mechanical behavior and bioinspired engineering. Dent Mater. 2017; 33:637–49. [PubMed: 28416222]
7. Zhang YR, Du W, Zhou XD, Yu HY. Review of research on the mechanical properties of the human tooth. Int J Oral Sci. 2014; 6:61–9. [PubMed: 24743065]
8. Labonte D, Lenz AK, Oyen ML. On the relationship between indentation hardness and modulus, and the damage resistance of biological materials. Acta Biomater. 2017
9. Kusakabe S, Rawls HR, Hotta M. Relationship between thin-film bond strength as measured by a scratch test, and indentation hardness for bonding agents. Dent Mater. 2016; 32:e55–62. [PubMed: 26777704]
10. Faria-e-Silva AL, De Moraes RR, de Menezes MS, Capanema RR, De Moura AS, Martelli H Jr. Hardness and microshear bond strength to enamel and dentin of permanent teeth with hypocalcified amelogenesis imperfecta. Int J Paediatr Dent. 2011; 21:314–20. [PubMed: 21470322]
11. Chun K, Choi H, Lee J. Comparison of mechanical property and role between enamel and dentin in the human teeth. J Dent Biomech. 2014; 5:1758736014520809. [PubMed: 24550998]
12. Xu C, Wang Y. Chemical composition and structure of peritubular and intertubular human dentine revisited. Arch Oral Biol. 2012; 57:383–91. [PubMed: 21996490]
13. Gallagher RR, Balooch M, Balooch G, Wilson RS, Marshall SJ, Marshall GW. Coupled Nanomechanical and Raman Microspectroscopic Investigation of Human Third Molar DEJ. J Dent Biomech. 2010; 1:1–8.
14. Idkaidek A, Agarwal V, Jasiuk I. Finite element simulation of Reference Point Indentation on bone. J Mech Behav Biomed Mater. 2017; 65:574–83. [PubMed: 27721174]
15. Toledano M, Osorio E, Aguilera FS, Cabello I, Toledano-Osorio M, Osorio R. Ex vivo detection and characterization of remineralized carious dentin, by nanoindentation and single point Raman spectroscopy, after amalgam restoration. Journal of Raman Spectroscopy. 2017; 48:384–92.
16. Toledano M, Aguilera FS, Osorio E, Cabello I, Toledano-Osorio M, Osorio R. Functional and molecular structural analysis of dentine interfaces promoted by a Zn-doped self-etching adhesive

and an in vitro load cycling model. J Mech Behav Biomed Mater. 2015; 50:131–49. [PubMed: 26122790]

17. Karan K, Yao X, Xu C, Wang Y. Chemical profile of the dentin substrate in non-carious cervical lesions. Dent Mater. 2009; 25:1205–12. [PubMed: 19464050]
18. Toledano M, Osorio R, Osorio E, Medina-Castillo AL, Toledano-Osorio M, Aguilera FS. Ions-modified nanoparticles affect functional remineralization and energy dissipation through the resin-dentin interface. J Mech Behav Biomed Mater. 2017; 68:62–79. [PubMed: 28152444]
19. Gutiérrez-Salazar, MdP, Reyes-Gasga, J. Microhardness and chemical composition of human tooth. Materials Research. 2003; 6:367–73.
20. Chuenarrom C, Benjakul P, Daosodsai P. Effect of indentation load and time on knoop and vickers microhardness tests for enamel and dentin. Materials Research. 2009; 12:473–6.
21. Halgaš R, Dusza J, Kaiferova J, Kovacsova L, Markovska N. Nanoindentation testing of human enamel and dentin. Ceramics–Silikáty. 2013; 57:92–9.
22. Fuentes V, Toledano M, Osorio R, Carvalho RM. Microhardness of superficial and deep sound human dentin. J Biomed Mater Res A. 2003; 66:850–3. [PubMed: 12926037]
23. Lai G, Zhu L, Xu X, Kunzelmann KH. An in vitro comparison of fluorescence-aided caries excavation and conventional excavation by microhardness testing. Clin Oral Investig. 2014; 18:599–605.
24. Shahdad SA, McCabe JF, Bull S, Rusby S, Wassell RW. Hardness measured with traditional Vickers and Martens hardness methods. Dent Mater. 2007; 23:1079–85. [PubMed: 17141860]
25. Toledano M, Osorio R, Osorio E, Garcia-Godoy F, Toledano-Osorio M, Aguilera FS. Advanced zinc-doped adhesives for high performance at the resin-carious dentin interface. J Mech Behav Biomed Mater. 2016; 62:247–67. [PubMed: 27232828]
26. Wang C, Wang Y, Huffman NT, Cui C, Yao X, Midura S, et al. Confocal laser Raman microspectroscopy of biomineralization foci in UMR 106 osteoblastic cultures reveals temporally synchronized protein changes preceding and accompanying mineral crystal deposition. J Biol Chem. 2009; 284:7100–13. [PubMed: 19116206]
27. Salehi H, Terrer E, Panayotov I, Levallois B, Jacquot B, Tassery H, et al. Functional mapping of human sound and carious enamel and dentin with Raman spectroscopy. Journal of biophotonics. 2013; 6:765–74. [PubMed: 22996995]
28. Freeman JJ, Wopenka B, Silva MJ, Pasteris JD. Raman Spectroscopic Detection of Changes in Bioapatite in Mouse Femora as a Function of Age and In Vitro Fluoride Treatment. Calcif Tissue Int. 2001; 68:156–62. [PubMed: 11351499]
29. Xu C, Reed R, Gorski J, Wang Y, Walker M. The distribution of carbonate in enamel and its correlation with structure and mechanical properties. Journal of materials science. 2012; 47:8035–43. [PubMed: 25221352]
30. Schwartz AG, Pasteris JD, Genin GM, Daulton TL, Thomopoulos S. Mineral distributions at the developing tendon enthesis. PloS one. 2012; 7:e48630. [PubMed: 23152788]
31. Pucéat E, Reynard B, Lécuyer C. Can crystallinity be used to determine the degree of chemical alteration of biogenic apatites? Chem Geol. 2004; 205:83–97.

HIGHLIGHTS

- BioDent RPI yields more consistent dentin hardness values compared to Knoop tester
- BioDent affected less by dentin elastic recovery and surface conditions than Knoop
- Raman spectroscopic results correlate with dentin microstructure and hardness
- Reduced dentin hardness is associated with less mineral and more carbonate content

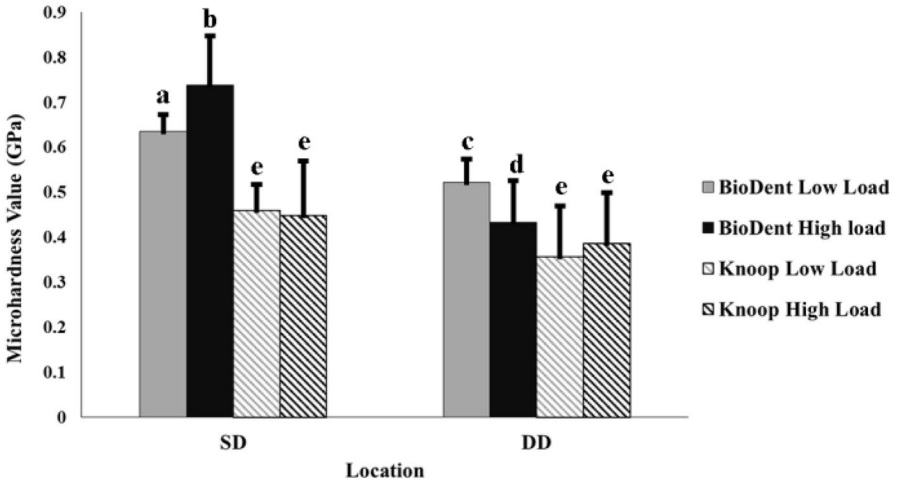

Figure 1.

Mean hardness values of dentin at two regions: Superficial dentin (SD) and deep dentin (DD). Mean values were calculated based on 10 indents per load per location on respective sections for each technique. Grey color represents low load level and black color represents high load level. Different letters indicate statistically significant differences within and between the two locations in dentin ($P<0.05$).

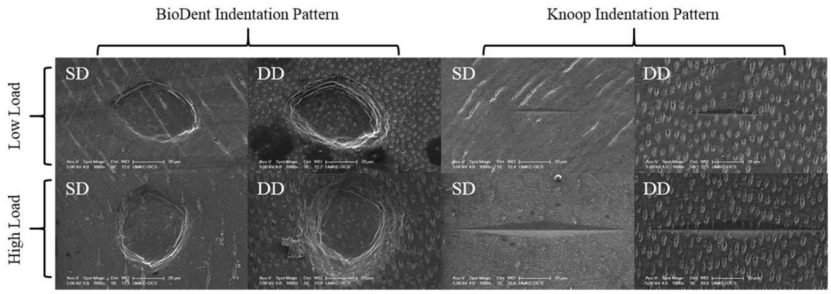

Figure 2.

SEM images of microindentation patterns in superficial dentin (SD) and deep dentin (DD) at high and low loads with BioDent RPI and Knoop hardness tests.

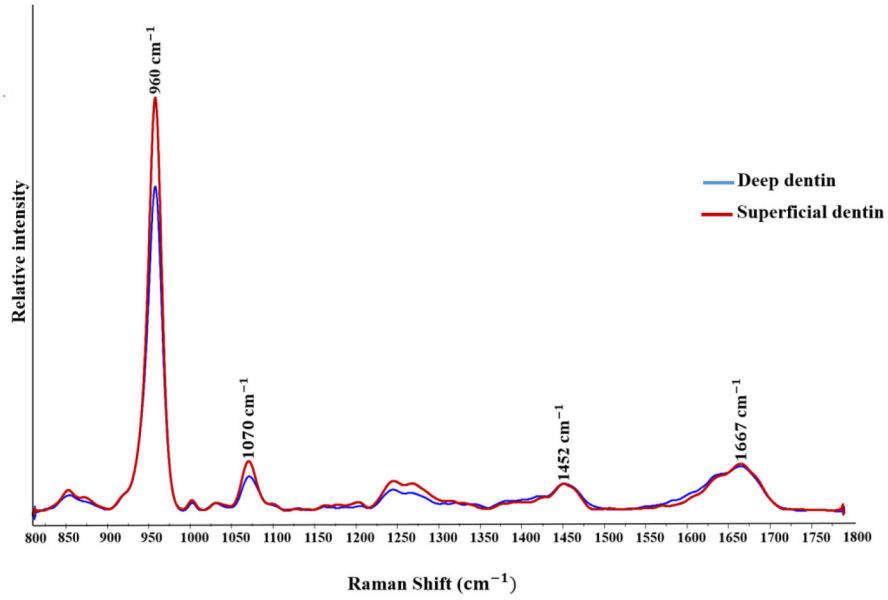

Figure 3.

Representative Raman spectra of deep dentin and superficial dentin in the range from 800 to 1800cm^{-1}. Spectra were normalized based on δ vibration of C-H band at 1452 cm^{-1}.

Table 1

Relative Raman intensity of phosphate peak at 960 cm^{-1} to the various peaks in the region of 800–1800 cm^{-1} and full-width-half maximum (FWHM) of phosphate peak width from deep dentin and superficial dentin.

	Superficial dentin Mean± SD	Deep dentin Mean± SD
$R_{960/1452}$	16.73 ± 1.75[a]	16.39 ± 1.62[a]
$R_{960/1667}$	3.48 ± 0.45[b]	2.99 ± 0.12[c]
$R_{960/1070}$	10.65 ± 1.13[d]	7.69 ± 1.26[e]
$FWHM_{960}$	18.26 ± 0.32[f]	19.16 ± 0.20[g]

Different superscript letters indicate statistically significant difference between superficial and deep dentin ($P<0.05$) within each measurement category.